

AP: Selective Activation for De-sparsifying Pruned Neural Networks

Shiyu Liu, Rohan Ghosh, Dylan Tan, Mehul Motani

Department of Electrical and Computer Engineering
School of Engineering, National University of Singapore
shiyu.liu@u.nus.edu, rghosh92@gmail.com, eledt@nus.edu.sg, motani@nus.edu.sg

Abstract

The rectified linear unit (ReLU) is a highly successful activation function in neural networks as it allows networks to easily obtain sparse representations, which reduces overfitting in overparameterized networks. However, in network pruning, we find that the sparsity introduced by ReLU, which we quantify by a term called dynamic dead neuron rate (DNR), is not beneficial for the pruned network. Interestingly, the more the network is pruned, the smaller the dynamic DNR becomes during optimization. This motivates us to propose a method to explicitly reduce the dynamic DNR for the pruned network, i.e., de-sparsify the network. We refer to our method as Activating-while-Pruning (AP). We note that AP does not function as a stand-alone method, as it does not evaluate the importance of weights. Instead, it works in tandem with existing pruning methods and aims to improve their performance by selective activation of nodes to reduce the dynamic DNR. We conduct extensive experiments using popular networks (e.g., ResNet, VGG) via two classical and three state-of-the-art pruning methods. The experimental results on public datasets (e.g., CIFAR-10/100) suggest that AP works well with existing pruning methods and improves the performance by 3% - 4%. For larger scale datasets (e.g., ImageNet) and state-of-the-art networks (e.g., vision transformer), we observe an improvement of 2% - 3% with AP as opposed to without. Lastly, we conduct an ablation study to examine the effectiveness of the components comprising AP.

1 Introduction

The rectified linear unit (ReLU) (Glorot, Bordes, and Bengio 2011), $\sigma(x) = \max\{x, 0\}$, is the most widely used activation function in neural networks (e.g., ResNet (He et al. 2016), Transformer (Vaswani et al. 2017)). The success of ReLU is mainly due to fact that existing networks tend to be overparameterized and ReLU can easily regularize overparameterized networks by introducing sparsity (i.e., post-activation output is zero) (Glorot, Bordes, and Bengio 2011), leading to promising results in many computer vision tasks (e.g., image classification (Simonyan and Zisserman 2014; He et al. 2016), object detection (Dai et al. 2021; Joseph et al. 2021)).

In this paper, we study the ReLU’s sparsity constraint in the context of network pruning (i.e., a method of compression that removes weights from the network). Specifically, we question the utility of ReLU’s sparsity constraint, when

the network is no longer overparameterized during iterative pruning. In the following, we summarize the workflow of our study together with our contributions.

1. **Motivation and Theoretical Study.** In Section 3.1, we introduce a term called dynamic Dead Neuron Rate (DNR), which quantifies the sparsity introduced by ReLU neurons that are not completely pruned during iterative pruning. Through rigorous experiments on popular networks (e.g., ResNet (He et al. 2016)), we find that the more the network is pruned, the smaller the dynamic DNR becomes during optimization. This suggests that the sparsity introduced by ReLU is not beneficial for pruned networks. Further theoretical investigations also reveal the importance of reducing dynamic DNR for pruned networks from an information bottleneck (IB) (Tishby and Zaslavsky 2015) perspective (see Sec. 3.2).
2. **A Method for De-sparsifying Pruned Networks.** In Section 3.3, we propose a method called Activating-while-Pruning (AP) which aims to explicitly reduce dynamic DNR. We note that AP does not function as a stand-alone method, as it does not evaluate the importance of weights. Instead, it works in tandem with existing pruning methods and aims to improve their performance by reducing dynamic DNR. The proposed AP has two variants: (i) AP-Lite which slightly improves the performance of existing methods, but without increasing the algorithm complexity, and (ii) AP-Pro which introduces an addition retraining step to the existing methods in every pruning cycle, but significantly improves the performance of existing methods.
3. **Experiments.** In Section 4, we conduct experiments on CIFAR-10/100 (Krizhevsky et al. 2009) with several popular networks (e.g., ResNet, VGG) using two classical and three state-of-the-art (SOTA) pruning methods. The results demonstrate that AP works well with existing pruning methods and improve their performance by 3% - 4%. For the larger scale dataset (e.g., ImageNet (Deng et al. 2009)) and SOTA networks (e.g., vision transformer (Dosovitskiy et al. 2020)), we observe an improvement of 2% - 3% with AP as opposed to without.
4. **Ablation Study.** In Section 4.3, we carry out an ablation study to investigate and demonstrate the effectiveness of several key components that make up the proposed AP.

2 Background

Network pruning is a method used to reduce the size of the neural network, with its first work (LeCun et al. 1998) dating back to 1990. In terms of the pruning style, all existing methods can be divided into two classes: (i) **One-Shot Pruning** and (ii) **Iterative Pruning**. Assuming that we plan to prune $Q\%$ of the parameters of a trained network, a typical **pruning cycle** consists of three basic steps:

1. Prune $\eta\%$ of existing parameters based on given metrics.
2. Freeze pruned weights as zero.
3. Retrain the pruned network to recover the performance.

In One-Shot Pruning, η is set to Q and the parameters are pruned in one pruning cycle. While for Iterative Pruning, a much smaller portion of parameters (i.e., $\eta \ll Q$) are pruned per pruning cycle. The pruning process is repeated multiple times until $Q\%$ of parameters are pruned. As for performance, Iterative Pruning often results in better performance compared to One-Shot Pruning (Han et al. 2015; Frankle and Carbin 2019; Li et al. 2017). So far, existing works aim to improve the pruning performance by exploring either new pruning metrics or new retraining methods.

Pruning Metrics. Weight magnitude is the most popular approximation metric used to determine less useful connections; the intuition being that smaller magnitude weights have a smaller effect in the output, and hence are less likely to have an impact on the model outcome if pruned (He et al. 2020; Li et al. 2020a,b). Many works have investigated the use of weight magnitude as the pruning metric, i.e. (Han et al. 2015; Frankle and Carbin 2019). More recently, (Lee et al. 2020) introduced layer-adaptive magnitude-based pruning (LAMP) and attempts to prune weights based on a scaled version of the magnitude. (Park et al. 2020) proposed a method called Lookahead Pruning (LAP), which evaluates the importance of weights based on the impact of pruning on neighbor layers. Another popular metric used for pruning is via the gradient; the intuition being that weights with smaller gradients are less impactful in optimizing the loss function. Examples are (LeCun et al. 1998; Theis et al. 2018), where (LeCun et al. 1998) proposed using the second derivative of the loss function with respect to the parameters (i.e., the Hessian Matrix) as a pruning metric and (Theis et al. 2018) used Fisher information to approximate the Hessian Matrix. A recent work (Blalock et al. 2020) reviewed numerous pruning methods and suggested two classical pruning methods for performance evaluation:

1. **Global Magnitude:** Pruning weights with the lowest absolute value anywhere in the network.
2. **Global Gradient:** Pruning weights with the lowest absolute value of (weight \times gradient) anywhere in the network.

Retraining Methods. Another factor that significantly affects the pruning performance is the retraining method. According to (Han et al. 2015), Han et al. trained the unpruned network with a learning rate schedule and retrained the pruned network using a constant learning rate (i.e., often the final learning rate of the learning rate schedule). A recent work (Renda, Frankle, and Carbin 2019) proposed learning rate rewinding which used the same learning rate schedule to retrain the pruned network, leading to a better

pruning performance. More recently, (Liu, Tan, and Motani 2021) attempted to optimize the choice of learning rate (LR) during retraining and proposed a LR schedule called S-Cyc. They showed that S-Cyc could work well with various pruning methods, further improving the existing performance. Most notably, (Frankle and Carbin 2019) found that resetting the unpruned weights to their original values (known as **weight rewinding**) after each pruning cycle could lead to even higher performance than the original model. Some follow-on works (Zhou et al. 2019; Renda, Frankle, and Carbin 2019; Malach et al. 2020) investigated this phenomenon more precisely and applied this method in other fields (e.g., transfer learning (Mehta 2019), reinforcement learning and natural language processing (Yu et al. 2020)).

Other Works. In addition to works mentioned above, several other works also share some deeper insights on network pruning (Liu et al. 2019; Zhu and Gupta 2018; Liu, Simonyan, and Yang 2019; Wang et al. 2020). For example, (Liu, Simonyan, and Yang 2019) demonstrated that training from scratch on the right sparse architecture yields better results than pruning from pre-trained models. Similarly, (Wang et al. 2020) suggested that the fully-trained network could reduce the search space for the pruned structure. More recently, (Luo and Wu 2020) addressed the issue of pruning residual connections with limited data and (Ye et al. 2020) theoretically proved the existence of small subnetworks with lower loss than the unpruned network.

3 Activating-while-Pruning

In Section 3.1, we first conduct experiments to evaluate the DNR during iterative pruning. Next, in Section 3.2, we link the experimental results to theoretical studies and motivate Activating-while-Pruning (AP). In Section 3.3, we introduce the idea of AP and present its algorithm. Lastly, in Section 3.4, we illustrate how AP can improve on the performance of existing pruning methods.

3.1 Experiments on DNR

We study the state of the ReLU function during iterative pruning and introduce a term called Dead Neuron Rate (DNR), which is the percentage of dead ReLU neurons (i.e., a neuron with a post-ReLU output of zero) in the network averaged over all training samples when the network converges. Mathematically, the DNR can be written as

$$\text{DNR} = \frac{1}{n} \sum_{i=1}^n \frac{\# \text{ of dead ReLU neurons}}{\text{all neurons in the unpruned network}}, \quad (1)$$

where n is the number of training samples. We classify a dead neuron as either dynamically dead or statically dead. The **dynamically dead neuron** is a dead neuron in which not all of the weights have been pruned. Hence, it is not likely to be permanently dead and its state depends on its input. As an example, a neuron can be dead for a sample X, but it could be active (i.e., post-ReLU output > 0) for a sample Y. The DNR contributed by dynamically dead neurons is referred to as **dynamic DNR**. The **statically dead neuron** is a dead neuron in which all associated weights have been pruned. The DNR contributed by statically dead neurons is referred to as **static DNR**.

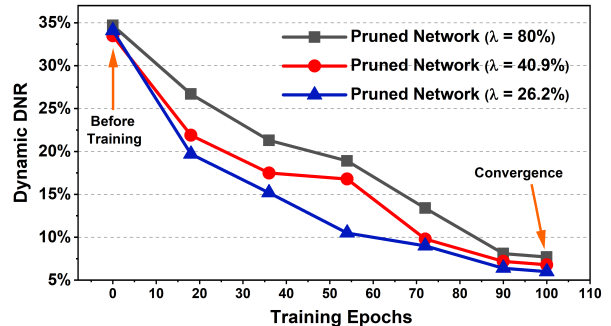
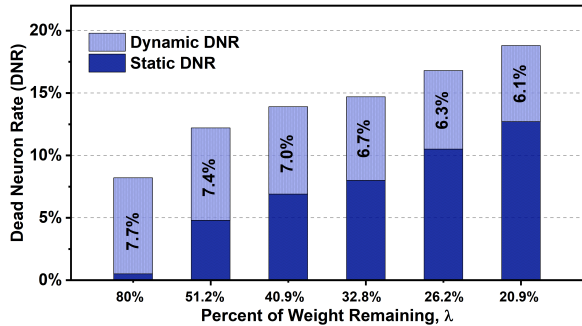


Figure 1: Dynamic and static Dead Neuron Rate (DNR) when iterative pruning ResNet-20 on CIFAR-10 using Global Magnitude. Left: dynamic and static DNR when the network converges; Right: dynamic DNR during optimization.

DNR is a term that we introduce to quantify the sparsity introduced by ReLU. Many similar sparsity metrics have been proposed in the literature (Hurley and Rickard 2009). As an example, the Gini Index (Goswami, Murthy, and Das 2016) computed from Lorenz curve (i.e., plot the cumulative percentages of total quantities) can be used to evaluate the sparsity of network graphs. Another popular metric will be Hoyer measure (Hoyer 2004) which is the ratio between L1 and L2 norms, can also be used to evaluate the sparsity of networks. The closest metric to DNR is parameter sparsity (Goodfellow, Bengio, and Courville 2016) which computes the percentage of zero-magnitude parameters among all parameters. We note that both parameter sparsity and DNR will contribute to sparse representations, and in this paper, we use DNR to quantify the sparsity introduced by ReLU.

Experiment Setup and Observations. Given the definition of DNR, static and dynamic DNR, we conduct pruning experiments using ResNet-20 on the CIFAR-10 dataset with the aim of examining the benefit (or lack thereof) of ReLU’s sparsity for pruned networks. We iteratively prune ResNet-20 with a pruning rate of 20 (i.e., 20% of existing weights are pruned) using the Global Magnitude (i.e., prune weights with the smallest magnitude anywhere in the network). We refer to the standard implementation reported in (Renda, Frankle, and Carbin 2019; Frankle and Carbin 2019) (i.e., SGD optimizer (Ruder 2016), 100 training epochs and batch size of 128, learning rate warmup to 0.03 and drop by a factor of 10 at 55 and 70 epochs) and compute the static DNR and dynamic DNR while the network is iteratively pruned. The experimental results are shown in Fig. 1, where we make two observations.

1. As shown in Fig. 1 (left), the value of DNR (i.e., sum of static and dynamic DNR) increases as the network is iteratively pruned. As expected, static DNR grows as more weights are pruned during iterative pruning.
2. Surprisingly, dynamic DNR tends to decrease as the network is iteratively pruned (see Fig. 1 (left)), suggesting that pruned networks do not favor the sparsity of ReLU. In Fig. 1 (right), we show that for pruned networks with different λ (i.e., percent of remaining weights), they have similar dynamic DNR before training, but the pruned network with smaller λ tends to have a smaller dynamic DNR during and after optimization.

Result Analysis. One possible reason for the decrease in dynamic DNR could be due to the fact that once the neuron is dead, its gradient becomes zero, meaning that it stops learning and degrades the learning ability of the network (Lu et al. 2019; Arnekvist et al. 2020). This could be beneficial as existing networks tend to be overparameterized and dynamic DNR may help to reduce the occurrence of overfitting. However, for pruned networks whose learning ability are heavily degraded, the dynamic DNR could be harmful as a dead ReLU always outputs the same value (zero as it happens) for any given non-positive input, meaning that it takes no role in discriminating between inputs. Therefore, during retraining, the pruned network attempts to restore its performance by reducing its dynamic DNR so that the extracted information can be passed to the subsequent layers. Similar performance trends can be observed using VGG-19 with Global Gradient (see Fig. 3 in the **Appendix**). Next, we present a **theoretical study** of DNR and show its relevance to the network’s ability to discriminate.

3.2 Relevance to IB and Complexity

Here, we present a theoretical result and subsequent insights that highlight the relevance of the dynamic DNR of a certain layer of the pruned network, to the Information Bottleneck (IB) Principle proposed in (Tishby and Zaslavsky 2015). In the IB setting, the computational flow is usually denoted by the graph $X \rightarrow T \rightarrow Y$, where X represents the input, T represents the extracted representation, and Y represents the network’s output. The IB principle states that the goal of training networks must be to minimize the mutual information (Cover and Thomas 2006) between X and T (denoted as $I(X; T)$) while keeping $I(Y; T)$ large. Overly compressed features (low $I(X; T)$) will not retain enough information to predict the labels, whereas under-compressed features (high $I(X; T)$) imply that more label-irrelevant information is retained in T which can adversely affect generalization. Next, we provide a few definitions.

Definition 1. Layer-Specific dynamic DNR ($D_{DNR}(T)$): We are given a dataset $S = \{X_1, \dots, X_m\}$, where $X_i \sim P \forall i$ and P is the data generating distribution. We denote the dynamic DNR of only the neurons at a certain layer within the network, represented by the vector T , by $D_{DNR}(T)$. $D_{DNR}(T)$ is computed over the entire distribution of input in P .

Definition 2. Layer-Specific static DNR ($S_{DNR}(T)$): It is defined in the same manner as $D_{DNR}(T)$, instead of computing the dynamic DNR, we compute the static DNR of T .

With this, we now outline our first theoretical result which highlights the relevance of $D_{DNR}(T)$ and $S_{DNR}(T)$ to $I(X; T)$, as follows.

Theorem 1. We are given the computational flow $X \rightarrow T \rightarrow Y$, where T represents the features at some arbitrary depth within a network, represented with finite precision (e.g. float32 or float64). We only consider the subset of network configurations for which (a) the activations in T are less than a threshold τ and (b) the zero-activation probability of each neuron in T is upper bounded by some $p_S < 1$. Let $dim(T)$ represent the dimensionality of T , i.e., the number of neurons at that depth. We then have,

$$I(X; T) \leq C \times dim(T) \times \left(1 - S_{DNR}(T) - D_{DNR}(T) \left(1 - \frac{1}{C} \log \frac{1 - S_{DNR}(T)}{D_{DNR}(T)} \right) \right), \quad (2)$$

for a finite constant C that only depends on the network architecture, τ and p_S .

The following corollary addresses the dependencies of Theorem 1. The proof of Theorem 1 and Corollary 1 are provided in the Appendix.

Corollary 1. The upper bound for $I(X; T)$ in Theorem 1 decreases in response to increase of $D_{DNR}(T)$ and $S_{DNR}(T)$.

Remark 1. (Relevance to Complexity) We see that (Shamir, Sabato, and Tishby 2010) notes how the metric $I(X; T)$ represents the *effective complexity* of the network. As Theorem 3 in (Shamir, Sabato, and Tishby 2010) shows, $I(X; T)$ captures the dependencies between X and T and directly correlates with the network’s function fitting ability. Coupled with the observations from Theorem 1 and Corollary 1, for a fixed pruned network configuration (i.e., fixed $S_{DNR}(T)$), greater $D_{DNR}(T)$ will likely reduce the *effective complexity* of the network, undermining the learning ability of the neural network.

Remark 2. (Motivation for AP) Theorem 1 also shows that a pruned network, which possesses large $S_{DNR}(T)$, leads to a higher risk of *over-compression* of information (low $I(X; T)$). To address this issue, we can reduce the dynamic DNR (from Corollary 1) so that the upper bound of $I(X; T)$ can be increased, mitigating the issue of *over-compression* for a pruned network. This agrees with our initial motivation that the sparsity introduced by ReLU is not beneficial for the pruned network and reducing dynamic DNR helps to improve the learning ability of the pruned network.

3.3 Algorithm of Activating-while-Pruning

The experimental and theoretical results above suggest that, in order to better preserve the learning ability of pruned networks, a smaller dynamic DNR is preferred. This motivates us to propose Activating-while-Pruning (AP) which aims to explicitly reduce dynamic DNR.

We note that the proposed AP does not work alone, as it does not evaluate the importance of weights. Instead, it

serves as a booster to existing pruning methods and help to improve their pruning performance by reducing dynamic DNR (see Fig. 2). Assume that the pruning method X removes $p\%$ of weights in every pruning cycle (see the upper part in Fig. 2). After using AP, the overall pruning rate remains unchanged as $p\%$, but $(p - q)\%$ of weights are pruned according to the pruning method X with the aim of pruning less important weights, while $q\%$ of weights are pruned according to AP (see the lower part in Fig. 2) with the aim of reducing dynamic DNR. Consider a network $f(\theta)$ with ReLU activation function. Two key steps to reducing dynamic DNR are summarized as follows.

(1) Locate Dead ReLU Neurons. Consider a neuron in the hidden layer with ReLU activation function, taking n inputs $\{X_1 W_1, \dots, X_n W_n | X_i \in \mathbb{R}$ is the input and $W_i \in \mathbb{R}$ is the associated weight}. Let j be the pre-activated output of the neuron (i.e., $j = \sum_{i=1}^n X_i W_i$) and \mathcal{J} be the post-activated output of the neuron ($\mathcal{J} = ReLU(j)$). Let \mathcal{L} be the loss function and assume the neuron is dead ($\mathcal{J} = 0$), then the gradient of its associated weights (e.g., W_1) with respect to the loss function will be $\frac{\partial \mathcal{L}}{\partial W_1} = \frac{\partial \mathcal{L}}{\partial \mathcal{J}} \cdot \frac{\partial \mathcal{J}}{\partial j} \cdot \frac{\partial j}{\partial W_1} = 0$ as $\frac{\partial \mathcal{J}}{\partial j} = 0$. If a neuron is often dead during training, the weight movement of its associated weights is likely to be smaller than other neurons. Therefore, we compute the difference between weights at initialization (θ_0) and the weights when the network converges (θ_*), i.e., $|\theta_* - \theta_0|$ and use it as a heuristic to locate dead ReLU neurons.

(2) Activate Dead ReLU Neurons. Assume we have located a dead neuron in the hidden layer with n inputs $\{X_1 W_1, \dots, X_n W_n | X_i \in \mathbb{R}$ is the input and $W_i \in \mathbb{R}$ is the associated weight}. We note that X_i is non-negative as X_i is usually the post-activated output from the previous layer (i.e., the output of ReLU is non-negative). Therefore, a straightforward way to activate the dead neuron is to prune the weights with the negative value. By pruning such negative weights, we can increase the value of the pre-activation output, which may turn the the pre-activation output into positive so as to reduce dynamic DNR.

3.4 How AP Improves Existing Methods

We now summarize how AP can improve existing pruning methods in Algorithm 2, where the upper part is the algorithm of a standard iterative pruning method called pruning method X and the lower part is the algorithm of method X with AP. The proposed AP has two variants: **AP-Pro** and **AP-Lite**. We note that both AP-Pro and AP-Lite contain the same three steps, summarized as follows.

- 1. Pruning.** Given a network at convergence with a set of dynamically dead ReLU neurons, $\mathcal{N}_1 = \{n_1, n_2, n_3, \dots\}$. The pruning step of AP aims to activate these dynamically dead ReLU neurons (i.e., reduce dynamic DNR) so as to preserve the learning ability of the pruned network (see the pruning metric of AP in algorithm 1).
- 2. Weight Rewinding.** Resetting unpruned weights to their values at the initialization. We note that different weight initializations could lead to different sets of \mathcal{N} . In the previous step, AP aims to reduce dynamic DNR for the target \mathcal{N}_1 and weight rewinding attempts to prevent the

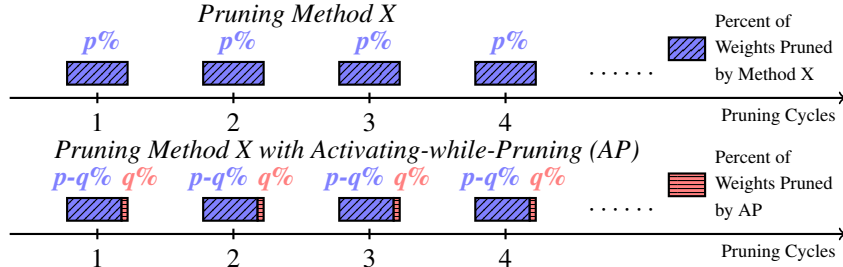


Figure 2: Illustration of how AP works in tandem with existing pruning methods (e.g., method X) in each pruning cycle.

Algorithm 1: The Pruning Metric of the Proposed AP

Require: (i) Network f with unpruned weights θ_0 at initialization, $f(\theta_0)$; (ii) Network f with unpruned weights θ_* at convergence, $f(\theta_*)$; (iii) Pruning Rate of AP, q ;

- 1: **Locate Dead Neurons:** Sort $|\theta_* - \theta_0|$ in an ascending order.
 - 2: **Activate Dead Neurons:** In the ascending order of $|\theta_* - \theta_0|$, prune first $q\%$ of weights with the negative magnitude.
-

target \mathcal{N}_1 from changing too much. Since the weights of ReLU neurons in \mathcal{N}_1 have been pruned by AP, these neurons could become active during retraining. The effect of weight rewinding is evaluated via an ablation study.

3. **Retraining** the pruned network to recover performance.

The key difference between AP-Lite and AP-Pro is that AP-Lite applies these three steps only once at the end of pruning (i.e., when all pruning cycles ends). It aims to slightly improve the performance, but does not substantially increase the algorithm complexity. For AP-Pro, it applies the three steps above in every pruning cycle, which increases the algorithm complexity (mainly due to the retraining step), but aims to significantly improve the performance, which could be preferred in performance oriented tasks.

4 Performance Evaluation

4.1 Experiment Setup

(1) **Experiment Details.** To demonstrate that AP can work well with different pruning methods, we shortlist two classical and three state-of-the-art pruning methods. The details for each experiment are summarized as follows.

1. Pruning ResNet-20 on the CIFAR-10 dataset using Global Magnitude with and without AP.
2. Pruning VGG-19 on the CIFAR-10 dataset using Global Gradient with and without AP.
3. Pruning DenseNet-40 (Huang et al. 2017) on CIFAR-100 using Layer-Adaptive Magnitude-based Pruning (LAMP) (Lee et al. 2020) with and without AP.
4. Pruning MobileNetV2 (Sandler et al. 2018) on the CIFAR-100 dataset using Lookahead Pruning (LAP) (Park et al. 2020) with and without AP.
5. Pruning ResNet-50 (He et al. 2016) on the ImageNet (i.e., ImageNet-1000) using Iterative Magnitude Pruning (IMP) (Frankle and Carbin 2019) with and without AP.
6. Pruning Vision Transformer (ViT-B-16) on CIFAR-10 using IMP with and without AP.

Algorithm 2: The Pruning Method X with and without AP

Require: (i) Network, $f(\theta)$; (ii) Pruning Rate of Method X, p ; (iii) Pruning Rate of AP, q ; (iv) Pro.Flag = {0: AP-Lite, 1: AP-Pro}; (v) Pruning Cycles, n ;

Pruning Method X

- 1: **for** $i = 1$ to n **do**
- 2: Randomly initialize unpruned weights, $\theta \leftarrow \theta_0$.
- 3: Train the network to convergence, arriving at parameters θ_* .

- 4: Prune $p\%$ of θ_* according to the pruning method X.
- 5: **end for**
- 6: Retrain the network to recover its performance.

Pruning Method X with Proposed AP

- 7: **for** $i = 1$ to n **do**
 - 8: Randomly initialize unpruned weights, $\theta \leftarrow \theta_0$.
 - 9: Train the network to convergence, arriving at parameters θ_* .
 - 10: Prune $(p - q)\%$ of θ_* according to the pruning method X.
 - 11: **if** Pro.Flag **then** # Execution of AP-Pro
 - 12: (i) *Pruning: Prune $q\%$ of parameter θ_* according to the metric of AP (see details in Algorithm 1).*
 - 13: (ii) *Weight Rewinding: Reset the remaining parameters to their values in θ_0 .*
 - 14: (iii) *Retrain: Retrain the pruned network to recover its performance.*
 - 15: **end if**
 - 16: **end for**
 - 17: **if** NOT Pro.Flag **then** # Execution of AP-Lite
 - 18: (i) *Pruning: Prune $q\%$ of the parameters θ_* according to the metric of AP (see details in Algorithm 1).*
 - 19: (ii) *Weight Rewinding: Reset the remaining parameters to their values in θ_0 .*
 - 20: (iii) *Retrain: Retrain the pruned network to recover its performance.*
 - 21: **end if**
-

We train the network using SGD with momentum = 0.9 and a weight decay of $1e-4$ (same as (Renda, Frankle, and Carbin 2019; Frankle and Carbin 2019)). For the benchmark pruning method, we prune the network with a pruning rate $p = 20$ (i.e., 20% of existing weights are pruned) in 1 pruning cycle. After using AP, the overall pruning rate remains unchanged as 20%, but 2% of existing weights are pruned based on AP, while the other 18% of existing weights are pruned based on the benchmark pruning method to be compared with (see Algorithm 2). We repeat 25 pruning cycles in 1 run and use the early-stop top-1 test accuracy (i.e., the corresponding test accuracy when early stopping criteria for validation error is met) to evaluate the performance. The ex-

Original Top-1 Test Accuracy: 91.7% ($\lambda = 100\%$)				
λ	32.8%	26.2%	13.4%	5.72%
Glob Mag	90.3 \pm 0.4	89.8 \pm 0.6	88.2 \pm 0.7	81.2 \pm 1.1
AP-Lite	90.4 \pm 0.7	90.2 \pm 0.8	88.7 \pm 0.7	82.4 \pm 1.4
AP-Pro	90.7\pm0.6	90.4\pm0.4	89.3\pm0.8	84.1\pm1.1

Table 1: Performance (top-1 test accuracy \pm standard deviation) of pruning ResNet-20 on CIFAR-10 using Global Magnitude (Glob Mag) with and without AP.

Original Top-1 Test Accuracy: 92.2% ($\lambda = 100\%$)				
λ	32.8%	26.2%	13.4%	5.72%
Glob Grad	90.2 \pm 0.5	89.8 \pm 0.8	89.2 \pm 0.8	76.9 \pm 1.1
AP-Lite	90.5 \pm 0.8	90.3 \pm 0.7	89.7 \pm 0.9	78.4 \pm 1.4
AP-Pro	90.8\pm0.6	90.7\pm0.9	90.4\pm0.8	79.2\pm1.3

Table 2: Performance (top-1 test accuracy \pm standard deviation) of pruning VGG-19 on CIFAR-10 using Global Gradient (Glob Grad) with and without AP.

perimental results averaged over 5 runs and the corresponding standard deviation are summarized in Tables 1 - 6, where λ is the percentage of weights remaining.

(2) Hyper-parameter Selection and Tuning. To ensure fair comparison against prior results, we utilize standard implementations (i.e., network hyper-parameters and learning rate schedules) reported in the literature. Specifically, the implementations for Tables 1 - 6 are from (Frankle and Carbin 2019), (Zhao et al. 2019), (Chin et al. 2020), (Renda, Frankle, and Carbin 2019) and (Dosovitskiy et al. 2020). The implementation details can be found in Section B.2 of the **Appendix**. In addition, we also tune hyper-parameters using the validation dataset via grid search. Some hyper-parameters are tuned as follows. (i) The training batch size is tuned from {64, 128, ..., 1024}. (ii) The learning rate is tuned from $1e-3$ to $1e-1$ via a stepsize of $2e-3$. (iii) The number training epochs is tuned from 80 to 500 with a stepsize of 20. The validation performance using our tuned parameters are close to that of using standard implementations. Therefore, we use standard implementations reported in the literature to reproduce benchmark results.

(3) Reproducing Benchmark Results. By using the implementations reported in the literature, we have correctly reproduced the benchmark results. For example, the benchmark results in our Tables 1 - 6 are comparable to Fig.11 and Fig.9 of (Blalock et al. 2020), Table.4 in (Liu et al. 2019), Fig.3 in (Chin et al. 2020), Fig. 10 in (Frankle et al. 2020), Table 5 in (Dosovitskiy et al. 2020), respectively.

(4) Source Code & Devices: We use Tesla V100 devices for our experiments and the source code (including random seeds) will be released at the camera-ready stage.

4.2 Performance Comparison

(1) Performance using SOTA and Classical Pruning Methods. In Tables 3 and 4, we show that AP can work well with SOTA pruning methods (e.g., LAMP, LAP). In Table 3, we show the performance of AP using LAMP via

Original Top-1 Test Accuracy: 74.6% ($\lambda = 100\%$)				
λ	32.8%	26.2%	13.4%	5.72%
LAMP	71.5 \pm 0.7	69.6 \pm 0.8	65.8 \pm 0.9	61.2 \pm 1.4
AP-Lite	71.9 \pm 0.8	70.3 \pm 0.7	66.6 \pm 0.7	62.2 \pm 1.2
AP-Pro	72.2\pm0.7	71.1\pm0.7	68.8\pm0.9	63.5\pm1.5

Table 3: Performance (top-1 test accuracy \pm standard deviation) of pruning DenseNet-40 on CIFAR-100 using Layer-Adaptive Magnitude Pruning (LAMP) with/without AP.

Original Top-1 Test Accuracy: 73.7% ($\lambda = 100\%$)				
λ	32.8%	26.2%	13.4%	5.72%
LAP	72.1 \pm 0.8	70.5 \pm 0.9	67.3 \pm 0.8	64.8 \pm 1.5
AP-Lite	72.5 \pm 0.9	70.9 \pm 0.8	68.2 \pm 1.2	66.2 \pm 1.5
AP-Pro	72.8\pm0.7	71.4\pm0.8	69.1\pm0.8	67.4\pm1.1

Table 4: Performance (top-1 test accuracy \pm standard deviation) of pruning MobileNetV2 on CIFAR-100 using Lookahead Pruning (LAP) with and without AP.

DenseNet-40 on CIFAR-100. We observe that AP-Lite improves the performance of LAMP by 1.2% at $\lambda = 13.4\%$ and the improvement increases to 1.6% at $\lambda = 5.7\%$. Note that AP-Lite does not increase the algorithm complexity of existing methods. For AP-Pro, it causes a larger improvement of 4.6% and 3.8% at $\lambda = 13.4\%$ and $\lambda = 5.7\%$, respectively. Similar performance trends can be observed in Table 4, where we show the performance of AP using LAP via MobileNetV2 on CIFAR-100. Furthermore, similar performance improvements can be observed using classical pruning methods (Global Magnitude/Gradient) via ResNet-20/VGG-19 on CIFAR-10 as well (see Tables 1 - 2).

(2) Performance on ImageNet. In Table 5, we show the performance of AP using Iterative Magnitude Pruning (IMP, i.e., the lottery ticket hypothesis pruning method) via ResNet-50 on ImageNet (i.e., the ILSVRC version) which contains over 1.2 million images from 1000 different classes. We observe that AP-Lite improves the performance of IMP by 1.5% at $\lambda = 5.7\%$. For AP-Pro, it improves the performance of IMP by 2.8% at $\lambda = 5.7\%$.

(3) Performance on SOTA networks (Vision Transformer). Several recent works (Liu et al. 2021; Yuan et al. 2021; Chen, Fan, and Panda 2021) demonstrated that transformer based networks tend to provide excellent performance in computer vision tasks (e.g., classification). We now examine the performance of AP using Vision Transformer (i.e., ViT-B16 with a resolution of 384). We note that the ViT-B16 uses Gaussian Error Linear Units (GELU, $\text{GELU}(x) = x\Phi(x)$, where $\Phi(x)$ is the standard Gaussian cumulative distribution function) as the activation function. Similar to ReLU which blocks the negative pre-activation output, GELU heavily regularizes the negative pre-activation output by multiplying an extremely small value of $\Phi(x)$, suggesting that AP could be helpful with pruning GELU based models as well.

We repeat the same experiment setup as above and evaluate the performance of AP using ViT-B16 in Table 6. We

Original Top-1 Test Accuracy: 77.0% ($\lambda = 100\%$)				
λ	32.8%	26.2%	13.4%	5.72%
IMP	76.8 \pm 0.2	76.4 \pm 0.3	75.2 \pm 0.4	71.5 \pm 0.4
AP-Lite	77.2 \pm 0.3	76.9 \pm 0.4	76.1 \pm 0.3	72.6 \pm 0.5
AP-Pro	77.5\pm0.4	77.2\pm0.3	76.8\pm0.6	73.5\pm0.4

Table 5: Performance (top-1 validation accuracy \pm standard deviation) of pruning ResNet-50 on ImageNet using Iterative Magnitude Pruning (IMP) with and without AP.

Original Top-1 Test Accuracy: 98.0% ($\lambda = 100\%$)				
λ	32.8%	26.2%	13.4%	5.72%
IMP	97.3 \pm 0.6	96.8 \pm 0.7	88.1 \pm 0.9	82.1 \pm 0.9
AP-Lite	98.0 \pm 0.4	97.3 \pm 0.7	89.9 \pm 0.6	83.6 \pm 0.8
AP-Pro	98.2\pm0.6	97.6\pm0.5	91.1\pm0.8	84.8\pm1.0

Table 6: Performance (top-1 test accuracy \pm standard deviation) of pruning Vision Transformer (ViT-B-16) on CIFAR-10 using IMP with and without AP.

observe that AP-Lite helps to improve the performance of IMP by 1.8% at $\lambda = 5.7\%$. For AP-Pro, it improves the performance of IMP by 3.3% at $\lambda = 5.7\%$.

4.3 Ablation Study

We now conduct an ablation study to evaluate the effectiveness of components in AP. Specifically, we remove one component at a time in AP and observe the impact on the pruning performance. We construct several variants of AP as follows.

- AP-Lite-NO-WR:** Using AP-Lite without the weight rewinding step (i.e., remove step (ii) from AP-Lite in Algorithm 2). This aims to evaluate the effect of weight rewinding on the pruning performance.
- AP-Lite-SOLO:** Using only AP-Lite without the benchmark pruning method (i.e., in every pruning cycle, pruning weights only based on AP). This aims to evaluate if the pruning metric of AP can be used to evaluate the importance of weights.

In Table 7, we conduct experiments of Pruning ResNet-20 on the CIFAR-10 dataset using Global Magnitude. Based on this configuration, we compare the performance of AP-Lite-NO-WR, AP-Lite-SOLO to AP-Lite so as to demonstrate the effectiveness of components in AP. We note that, same as above, we utilize the implementation reported in the literature. Specifically, the hyper-parameters and the learning rate schedule are from (Frankle and Carbin 2019).

Effect of Weight Rewinding. In Table 7, we compare the performance of AP-Lite-NO-WR to AP-Lite while the key difference is that AP-Lite utilizes weight rewinding (see Algorithm 2) and AP-Lite-NO-WR does not. We find that the performance of AP-Lite at $\lambda = 51.2\%$ is 2.4% higher than AP-Lite-NO-WR. It suggests the crucial role of weight rewinding in improving the performance. Similar performance trends can be observed for other values of λ .

When AP Works Solely. The pruning metric of AP (see algorithm 1) aims to reduce dynamic DNR by pruning. We

λ	51.2%	40.9%	32.8%
AP-Lite	89.6\pm0.5	88.9\pm0.6	88.5\pm0.8
AP-Lite-SOLO	87.1 \pm 0.7	86.3 \pm 0.9	85.2 \pm 1.1
AP-Lite-NO-WR	87.5 \pm 0.5	86.8 \pm 0.8	85.9 \pm 0.9

Table 7: Ablation Study: Performance Comparison (top-1 test accuracy \pm standard deviation) between AP-Lite and AP-SOLO, AP-Lite-NO-WR on pruning ResNet-20 on CIFAR-10 via Global Magnitude.

compare the performance of AP-Lite-SOLO to AP-Lite to evaluate if the pruning metric of AP can be used solely, without working with other pruning methods. In Table 7, we observe that AP-Lite-SOLO performs much worse than AP-Lite. For example, at $\lambda = 51.2\%$, the performance of AP-Lite-SOLO is 87.1, which is 2.8% lower than AP-Lite. Similar performance trends can be observed in Table 14 (see **Appendix**), where we prune VGG-19 using CIFAR-10. It suggests that the pruning metric of AP is not suitable to evaluate the importance of weights. The effect of AP’s metric on reducing dynamic DNR and its pruning rate q on pruning performance are discussed in the Reflections below.

5 Reflections

The proposed AP aims to improve existing pruning methods by reducing dynamic DNR. The extensive experiments on popular/SOTA networks and large-scale datasets demonstrate that AP works well with various pruning methods, significantly improving the performance by 3% - 4%. We now conclude the paper by presenting some relevant points.

(1) Pruning Rate of AP, q . AP removes $q\%$ of remaining parameters in every pruning cycle, so as to reduce dynamic DNR. The value of q is usually much smaller than the pruning rate of the pruning method it works with. Adjusting the value of q is a trade-off between pruning less important weights and reducing dynamic DNR. A large q indicates preferential reduction of dynamic DNR, while a small q means preferential removal of less important weights. We conduct experiments to evaluate the effect of q on the performance and results suggest that a smaller value of q could lead to good performance (see **Appendix** for more details).

(2) Dynamic DNR with AP. We also examine the effect of AP in reducing dynamic DNR. The experimental results on ResNet-20/VGG-19 suggest that AP works as expected and significantly reduce the dynamic DNR. We refer interested reader to **Appendix** for more details.

(3) Reducing Static DNR. The Theorem 1 shows that, in addition to dynamic DNR, reducing static DNR also can improve the upper bound of $I(X; T)$. In fact, reducing static DNR has been incorporated directly or indirectly into the existing pruning methods. As an example, LAMP (i.e., one SOTA pruning method used in performance evaluation, see Table 3) takes the number of unpruned weights of neurons/layers into account and avoids pruning weights from neurons/filters with less number of unpruned weights. This prevents neurons from being statically dead. Differ from existing methods, AP is the first method targeting the dynamic DNR. Hence, as a method that works in tandem with exist-

ing pruning methods, AP improves existing pruning methods by filling in the gap in reducing dynamic DNR, leading to much better pruning performance.

References

- Arnekvist, I.; Carvalho, J. F.; Kragic, D.; and Stork, J. A. 2020. The effect of Target Normalization and Momentum on Dying ReLU. *CoRR*, abs/2005.06195.
- Blalock, D.; et al. 2020. What is the State of Neural Network Pruning? In *Proceedings of the Machine Learning and Systems (MLSys)*.
- Chen, C.-F. R.; Fan, Q.; and Panda, R. 2021. Crossvit: Cross-attention multi-scale vision transformer for image classification. In *Proceedings of the IEEE/CVF International Conference on Computer Vision*, 357–366.
- Chin, T.-W.; Ding, R.; Zhang, C.; and Marculescu, D. 2020. Towards efficient model compression via learned global ranking. In *Proceedings of the IEEE/CVF Conference on Computer Vision and Pattern Recognition (CVPR)*, 1518–1528.
- Cover, T. M.; and Thomas, J. A. 2006. *Elements of Information Theory, 2nd edition*. John Wiley & Sons.
- Dai, X.; Chen, Y.; Xiao, B.; Chen, D.; Liu, M.; Yuan, L.; and Zhang, L. 2021. Dynamic head: Unifying object detection heads with attentions. In *Proceedings of the IEEE/CVF Conference on Computer Vision and Pattern Recognition*, 7373–7382.
- Deng, J.; et al. 2009. Imagenet: A large-scale hierarchical image database. In *2009 IEEE conference on computer vision and pattern recognition*, 248–255. IEEE.
- Dosovitskiy, A.; Beyer, L.; Kolesnikov, A.; Weissenborn, D.; Zhai, X.; Unterthiner, T.; Dehghani, M.; Minderer, M.; Heigold, G.; Gelly, S.; et al. 2020. An image is worth 16x16 words: Transformers for image recognition at scale. *arXiv preprint arXiv:2010.11929*.
- Frankle, J.; and Carbin, M. 2019. The Lottery Ticket Hypothesis: Finding Sparse, Trainable Neural Networks. In *Proceedings of the International Conference on Learning Representations (ICLR)*.
- Frankle, J.; Dziugaite, G. K.; Roy, D. M.; and Carbin, M. 2019. Stabilizing the lottery ticket hypothesis. *arXiv preprint arXiv:1903.01611*.
- Frankle, J.; et al. 2020. Linear Mode Connectivity and the Lottery Ticket Hypothesis. In *Proceedings of the International Conference on Machine Learning (ICML)*, 3259–3269.
- Glorot, X.; Bordes, A.; and Bengio, Y. 2011. Deep sparse rectifier neural networks. In *Proceedings of the fourteenth international conference on artificial intelligence and statistics*, 315–323. JMLR Workshop and Conference Proceedings.
- Goodfellow, I.; Bengio, Y.; and Courville, A. 2016. *Deep learning*. MIT press.
- Goswami, S.; Murthy, C. A.; and Das, A. K. 2016. Sparsity Measure of a Network Graph: Gini Index. *arXiv:1612.07074*.
- Han, S.; et al. 2015. Learning both weights and connections for efficient neural network. In *Proceedings of the Advances in Neural Information Processing Systems (Neurips)*, 1135–1143.
- He, K.; et al. 2016. Deep residual learning for image recognition. In *Proceedings of the IEEE Conference on Computer Vision and Pattern Recognition*, 770–778.
- He, Y.; Ding, Y.; Liu, P.; Zhu, L.; Zhang, H.; and Yang, Y. 2020. Learning filter pruning criteria for deep convolutional neural networks acceleration. In *Proceedings of the IEEE/CVF conference on computer vision and pattern recognition*, 2009–2018.
- Hoyer, P. O. 2004. Non-negative matrix factorization with sparseness constraints. *Journal of Machine Learning Research*, 5(9).
- Huang, G.; et al. 2017. Densely connected convolutional networks. In *Proceedings of the IEEE/CVF Conference on Computer Vision and Pattern Recognition*, 4700–4708.
- Hurley, N. P.; and Rickard, S. T. 2009. Comparing Measures of Sparsity. *arXiv:0811.4706*.
- Joseph, K.; Khan, S.; Khan, F. S.; and Balasubramanian, V. N. 2021. Towards open world object detection. In *Proceedings of the IEEE/CVF Conference on Computer Vision and Pattern Recognition*, 5830–5840.
- Krizhevsky, A.; et al. 2009. Learning multiple layers of features from tiny images.
- LeCun, Y.; et al. 1998. Gradient-based learning applied to document recognition. *Proceedings of the IEEE*, 86(11): 2278–2324.
- Lee, J.; Park, S.; Mo, S.; Ahn, S.; and Shin, J. 2020. Layer-adaptive Sparsity for the Magnitude-based Pruning. In *International Conference on Learning Representations (ICLR)*.
- Li, B.; Wu, B.; Su, J.; and Wang, G. 2020a. Eagleeye: Fast sub-net evaluation for efficient neural network pruning. In *European conference on computer vision*, 639–654. Springer.
- Li, H.; et al. 2017. Pruning filters for efficient convnets. In *Proceedings of the International Conference on Learning Representations (ICLR)*.
- Li, Y.; Wu, W.; Liu, Z.; Zhang, C.; Zhang, X.; Yao, H.; and Yin, B. 2020b. Weight-Dependent Gates for Differentiable Neural Network Pruning. In *European Conference on Computer Vision*, 23–37. Springer.
- Liu, H.; Simonyan, K.; and Yang, Y. 2019. DARTS: Differentiable architecture search. In *Proceedings of the International Conference on Learning Representations (ICLR)*.
- Liu, S.; Tan, C. M. J.; and Motani, M. 2021. S-Cyc: A Learning Rate Schedule for Iterative Pruning of ReLU-based Networks. *CoRR*, abs/2110.08764.
- Liu, Z.; Lin, Y.; Cao, Y.; Hu, H.; Wei, Y.; Zhang, Z.; Lin, S.; and Guo, B. 2021. Swin transformer: Hierarchical vision transformer using shifted windows. In *Proceedings of the IEEE/CVF International Conference on Computer Vision*, 10012–10022.

- Liu, Z.; et al. 2019. Rethinking the value of network pruning. In *Proceedings of the International Conference on Learning Representations (ICLR)*.
- Lu, L.; Shin, Y.; Su, Y.; and Karniadakis, G. E. 2019. Dying relu and initialization: Theory and numerical examples. *arXiv preprint arXiv:1903.06733*.
- Luo, J.-H.; and Wu, J. 2020. Neural Network Pruning with Residual-Connections and Limited-Data. In *Proceedings of the IEEE/CVF Conference on Computer Vision and Pattern Recognition (CVPR)*, 1458–1467.
- Malach, E.; et al. 2020. Proving the lottery ticket hypothesis: Pruning is all you need. In *Proceedings of the International Conference on Machine Learning (ICML)*, 6682–6691.
- Mehta, R. 2019. Sparse Transfer Learning via Winning Lottery Tickets. In *Proceedings of the Advances in Neural Information Processing Systems Workshop on Learning Transferable Skills*.
- Park, S.; Lee, J.; Mo, S.; and Shin, J. 2020. Lookahead: A far-sighted alternative of magnitude-based pruning.
- Renda, A.; Frankle, J.; and Carbin, M. 2019. Comparing rewinding and fine-tuning in neural network pruning. In *International Conference on Learning Representations (ICLR)*.
- Ruder, S. 2016. An overview of gradient descent optimization algorithms. *arXiv preprint arXiv:1609.04747*.
- Sandler, M.; Howard, A.; Zhu, M.; Zhmoginov, A.; and Chen, L.-C. 2018. Mobilenetv2: Inverted residuals and linear bottlenecks. In *Proceedings of the IEEE conference on computer vision and pattern recognition*, 4510–4520.
- Shamir, O.; Sabato, S.; and Tishby, N. 2010. Learning and generalization with the information bottleneck. *Theoretical Computer Science*, 411(29): 2696–2711.
- Simonyan, K.; and Zisserman, A. 2014. Very deep convolutional networks for large-scale image recognition. *arXiv preprint arXiv:1409.1556*.
- Theis, L.; et al. 2018. Faster gaze prediction with dense networks and fisher pruning. *arXiv preprint arXiv:1801.05787*.
- Tishby, N.; and Zaslavsky, N. 2015. Deep Learning and the Information Bottleneck Principle. *arXiv:1503.02406*.
- Vaswani, A.; Shazeer, N.; Parmar, N.; Uszkoreit, J.; Jones, L.; Gomez, A. N.; Kaiser, Ł.; and Polosukhin, I. 2017. Attention is all you need. In *Advances in neural information processing systems*, 5998–6008.
- Wang, Y.; et al. 2020. Pruning from scratch. In *Proceedings of the AAAI Conference on Artificial Intelligence*, volume 34, 12273–12280.
- Ye, M.; et al. 2020. Good subnetworks provably exist: Pruning via greedy forward selection. In *Proceedings of the International Conference on Machine Learning (ICML)*, 10820–10830. PMLR.
- Yu, H. n.; et al. 2020. Playing the lottery with rewards and multiple languages: lottery tickets in RL and NLP. In *Proceedings of the International Conference on Learning Representations (ICLR)*.
- Yuan, L.; Hou, Q.; Jiang, Z.; Feng, J.; and Yan, S. 2021. Volo: Vision outlooker for visual recognition. *arXiv preprint arXiv:2106.13112*.
- Zhao, C.; et al. 2019. Variational convolutional neural network pruning. In *Proceedings of the IEEE/CVF Conference on Computer Vision and Pattern Recognition (CVPR)*, 2780–2789.
- Zhou, H.; et al. 2019. Deconstructing Lottery Tickets: Zeros, Signs, and the Supermask. In *Proceedings of the Advances in Neural Information Processing Systems (Neurips)*.
- Zhu, M.; and Gupta, S. 2018. To prune, or not to prune: exploring the efficacy of pruning for model compression. In *Proceedings of the International Conference on Learning Representations (ICLR)*.

A Proofs of Theoretical Results

In this section, we provide the proofs for theoretical results (Theorem 1 and Corollary 1) of the main paper.

A.1 Proof of Theorem 1

Theorem 1. We are given the computational flow $X \rightarrow T \rightarrow Y$, where T represents the features at some arbitrary depth within a network, represented with finite precision (e.g. float32 or float64). We only consider the subset of network configurations for which (a) the activations in T are less than a threshold τ and (b) the zero-activation probability of each neuron in T is upper bounded by some $p_S < 1$. Let $\dim(T)$ represent the dimensionality of T , i.e., the number of neurons at that depth. We then have,

$$I(X; T) \leq C \times \dim(T) \times \left(1 - S_{DNR}(T) - D_{DNR}(T) \left(1 - \frac{1}{C} \log \frac{1 - S_{DNR}(T)}{D_{DNR}(T)} \right) \right), \quad (3)$$

for a finite constant C that only depends on the network architecture, τ and p_S .

Proof. First, note that due to finite precision T is a discrete variable, and thus $I(X; T) = H(T)$, as $T = f(X)$ is a deterministic function of X , where f denotes the function within the network that maps X to T . Next, let us only consider the nodes in T which are not statically dead; i.e. they do not form a part of the $S_{DNR}(T)$. Let us denote them as active nodes. Note that there will be $k = \dim(T) \times (1 - S_{DNR}(T))$ active nodes in this case.

For these k nodes, let p_1, p_2, \dots, p_k denote the probability that each node will be zero-valued, when X is drawn infinitely over the entire distribution P . Let us also denote $D'_{DNR}(T) = \frac{D_{DNR}(T)}{1 - S_{DNR}(T)}$ as the cardinality adjusted dynamic DNR rate of the pruned network. Note that $\mathbb{E}[p_i] = D'_{DNR}(T)$. Let us represent these k nodes by T_1, T_2, \dots, T_k for what follows. Note that like T , each T_i will be discrete valued. We can thus write

$$H(T) \leq \sum H(T_i) \quad (4)$$

□

As all activations are less than τ , if the precision of representation is α , we will have a maximum $N = \frac{\tau}{\alpha}$ number of possible outcomes for each T_i . Let $\phi_0^i, \phi_1^i, \dots, \phi_{N-1}^i$ thus represent the probabilities of T_i being each possible discrete outcome. We have that $\sum_j \phi_j^i = 1$. Note that $\phi_0^i = p_i$.

Now, we can write

$$H(T_i) = p_i \log \frac{1}{p_i} + (1 - p_i) \sum_{N-1 \geq j \geq 1} \frac{\phi_j^i}{(1 - p_i)} \log \frac{1}{\phi_j^i} \quad (5)$$

Here let us consider the quantity $\sum_{N-1 \geq j \geq 1} \frac{\phi_j^i}{(1 - p_i)} \log \frac{1}{\phi_j^i}$. Let C be the maximum possible value this quantity can take, across all network weight configurations that obey the constraints provided in the Theorem. Note that C will only depend on the network architecture, and the parameters τ and p_S . We will now demonstrate that C is finite, and provide an upper bound for the same.

Given $p_i = \phi_0^i$, we have that $\sum_{j \geq 1} \phi_j^i = 1 - p_i$. Thus, under this constant summation constraint, the quantity $\sum_{N-1 \geq j \geq 1} \frac{\phi_j^i}{(1 - p_i)} \log \frac{1}{\phi_j^i}$ will only be maximized when $\phi_1^i = \phi_2^i = \dots \phi_{N-1}^i = \frac{1 - p_i}{N - 1}$. Thus, we have

$$C \leq \sum_{N-1 \geq j \geq 1} \frac{1}{N - 1} \log \frac{N - 1}{1 - p_i} \quad (6)$$

$$= \log \frac{N - 1}{1 - p_i} \leq \log \frac{N - 1}{1 - p_S} \quad (7)$$

This shows that C is finite, and depends on the network architecture, p_S and τ (which affects N). Lastly, we have

$$\sum_{i=1}^k H(T_i) \leq \sum_{i=1}^k \left(p_i \log \frac{1}{p_i} + (1 - p_i) C \right) \quad (8)$$

$$= \sum_{i=1}^k p_i \log \frac{1}{p_i} + k \times C \times (1 - D'_{DNR}(T)) \quad (9)$$

$$\leq k \times D'_{DNR}(T) \log \frac{1}{D'_{DNR}(T)} + k \times C \times (1 - D'_{DNR}(T)) \quad (10)$$

$$= C \times \dim(T) (1 - S_{DNR}(T)) \left(1 - D'_{DNR}(T) \left(1 - \frac{1}{C} \log \frac{1}{D'_{DNR}(T)} \right) \right), \quad (11)$$

where the last step follows from the definition of k . Replacing $D'_{DNR}(T) = \frac{D_{DNR}(T)}{1-S_{DNR}(T)}$ yields the intended result.

A.2 Proof of Corollary 1

Corollary 1. The upper bound for $I(X; T)$ in Theorem 1 decreases in response to increase of both $D_{DNR}(T)$ and $S_{DNR}(T)$.

Proof. It is trivial to see that increasing $S_{DNR}(T)$ can only decrease the upper bound. Let us denote

$$Z = C \times \dim(T) (1 - S_{DNR}(T)) \left(1 - D'_{DNR}(T) \left(1 - \frac{1}{C} \log \frac{1}{D'_{DNR}(T)} \right) \right). \quad (12)$$

For simplicity of notation, let $\beta = C \times \dim(T) \times (1 - S_{DNR}(T))$. For investigating how the upper bound of $I(X; T)$ (denoted as Z) changes with $D_{DNR}(T)$, we first compute the derivative of Z w.r.t $D'_{DNR}(T)$ which yields the following expression.

$$\frac{dZ}{d(D'_{DNR}(T))} = \beta \left(- \left(1 - \frac{1}{C} \log \frac{1}{D'_{DNR}(T)} \right) - D'_{DNR}(T) \left(\frac{1}{C \times D'_{DNR}(T)} \right) \right) \quad (13)$$

$$= \beta \left(-1 - \frac{1}{C} + \frac{1}{C} \log \frac{1}{D'_{DNR}(T)} \right) \quad (14)$$

□

For $\frac{dZ}{d(D'_{DNR}(T))}$ to be less than or equal to 0, we must have

$$C \geq \log \frac{1}{D'_{DNR}(T)} - 1. \quad (15)$$

In what follows, we will show that $C \geq \log \frac{1}{D'_{DNR}(T)}$ itself. Please refer to the proof of Theorem 1 for the definitions.

For each node output represented in T_1, T_2, \dots, T_k , we add a negative bias of $-\frac{1}{\phi_j^i}$, and flip the sign of all the weights pointing to each of these nodes. We note that performing this change would yield that $\sum_{j=1}^{N-1} \phi_j^i = p_i$. We will then have that

$$\sum_{N-1 \geq j \geq 1} \frac{\phi_j^i}{(p_i)} \log \frac{1}{\phi_j^i} \geq \log \frac{1}{p_i}, \quad (16)$$

where the lower bound is achieved by only filling the remaining probability p_i onto a single bin. Now, as C represents the maximum possible value that the quantity bounded in (16) can take, we naturally have that $C \geq \log \frac{1}{p_i}$ as well, for all i . As $\mathbb{E}[p_i] = D'_{DNR}(T)$, it also then follows that $C \geq \log \frac{1}{D'_{DNR}(T)}$. This proves our intended result, and yields that $\frac{dZ}{d(D'_{DNR}(T))} \leq 0$.

Therefore, given that $D'_{DNR}(T) = \frac{D_{DNR}(T)}{1-S_{DNR}(T)}$, a larger value of both D_{DNR} and S_{DNR} will lead to a larger value of $D'_{DNR}(T)$, decreasing Z (i.e., the upper bound of $I(X; Z)$) and increasing the risk of *over-compression*.

B Supplementary Experimental Results

In the Appendix, we show some additional experimental results. Specifically,

1. In Section B.1, we repeat the DNR experiment using VGG-19 on the CIFAR-10 dataset with the Global Gradient pruning method.
2. In Section B.2, we present the implementation details used in the Section of Performance Evaluation (i.e., Section 4) and demonstrate the performance of AP for more values of λ .
3. In Section B.3, we show the ablation study results using VGG-19 on CIFAR-10 with the Global Gradient pruning method.
4. In Section B.4, we evaluate the effect of pruning rate, q , on the pruning performance using ResNet-20 and VGG-19 on the CIFAR-10 dataset.
5. In Section B.5, we evaluate the effect of AP on reducing the dynamic DNR on the pruning performance using ResNet-20 and VGG-19 on the CIFAR-10 dataset.

B.1 The dynamic DNR experiment

In this section, we repeat the DNR experiment in the Section of Activating-while-Pruning (i.e., Section 3) using VGG-19 on CIFAR-10 with global gradient pruning method. The hyper-parameters and the LR schedule used are from (Frankle and Carbin 2019). As shown in Fig. 3, we observe the performance trend largely mirrors those reported in Fig. 1. The dynamic DNR tends to decrease as the network is iteratively pruned (shown in Fig. 3 (left)), and during optimization, the network aims to reduce the dynamic DNR so as to preserve the learning ability of the pruned network.

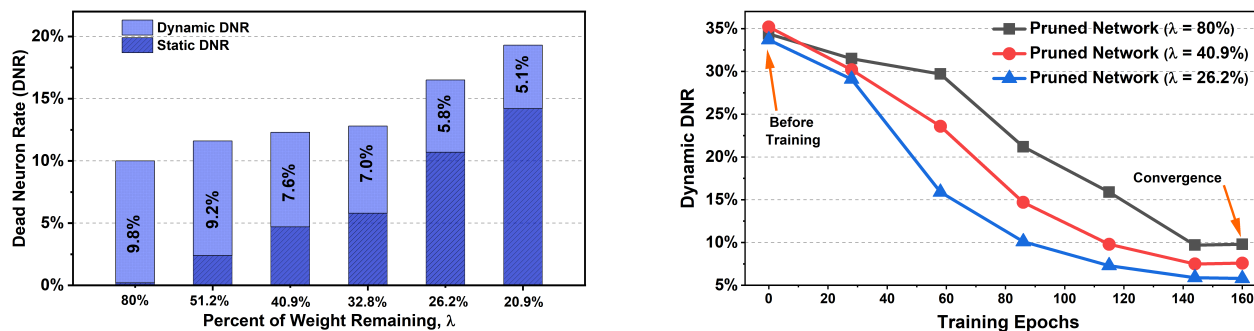


Figure 3: Dynamic and static Dead Neuron Rate (DNR) when iteratively pruning VGG-19 on CIFAR-10 using Global Gradient. Left: dynamic and static DNR when the network converges; Right: dynamic DNR during optimization.

B.2 Implementation Details and Performance of AP for More Values of λ

In this section, we present the implementation details used in the Section of Performance Evaluation (i.e., Section 4) and demonstrate the performance of AP for more values of λ .

(1) Implementation Details. We use standard implementations reported in the literature. Specifically, the implementation for Tables 8 - 9 is from (Frankle and Carbin 2019). The implementation for Table 10 - 13 are from (Zhao et al. 2019), (Chin et al. 2020), (Renda, Frankle, and Carbin 2019) and (Dosovitskiy et al. 2020), respectively. The implementation details can also be found on the top row of each table (from Table 8 to Table 13). Furthermore, for the IMP method examined in this work, we rewind the unpruned weights to their values during training (e.g., epoch 6), in order to obtain a more stable subnetwork (Frankle et al. 2019). To better work with IMP, the weight rewinding step in the proposed AP also rewinds the unpruned weights to their values during training (i.e., the same epoch as IMP).

(2) More Performance of AP. In Tables 8- 13, we also show performance of AP for more values of λ . We observe that for other values of λ , AP-Lite and AP-Pro also help to achieve higher performance. For example, in Table 9, AP-Lite improves the performance of the Global Gradient (at $\lambda = 8.59\%$) from 84.5% to 86.1% while AP-Pro improves the performance to 87.0%.

(i) Params: 270K; (ii) Train Steps: 100 Epochs; (iii) Batch size: 128; (iv) LR Schedule: warmup to 0.03 at 55 epochs, 10X drop at 55, 70 epochs.			
Percent of Weights Remaining	Global Magnitude	AP-Lite	AP-Pro
$\lambda = 100.0\%$	91.7 \pm 0.2	91.7 \pm 0.2	91.7 \pm 0.5
$\lambda = 64.0\%$	91.5 \pm 0.3	91.7 \pm 0.2	91.8\pm0.3
$\lambda = 40.9\%$	90.8 \pm 0.5	91.0 \pm 0.6	91.4\pm0.4
$\lambda = 32.8\%$	90.3 \pm 0.4	90.4 \pm 0.7	90.7\pm0.6
$\lambda = 26.2\%$	89.8 \pm 0.6	90.2 \pm 0.8	90.4\pm0.7
$\lambda = 13.4\%$	88.2 \pm 0.7	88.7 \pm 0.7	89.3\pm0.8
$\lambda = 8.59\%$	85.9 \pm 0.9	86.8 \pm 0.9	87.3\pm0.8
$\lambda = 5.72\%$	81.2 \pm 1.1	82.4 \pm 0.8	84.1\pm1.1

Table 8: Performance (top-1 test accuracy \pm standard deviation) of pruning ResNet-20 on CIFAR-10 using Global Magnitude with and without AP. The hyper-parameters and the LR schedule are from (Frankle and Carbin 2019).

(i) Params: 139M; (ii) Train Steps: 160 epochs; (iii) Batch size: 64; (iv) LR Schedule: warmup to 0.1 at 15 epochs, 10X drop at 85, 125 epochs.			
Percent of Weights Remaining	Global Gradient	AP-Lite	AP-Pro
$\lambda = 100.0\%$	92.2 \pm 0.3	92.2 \pm 0.3	92.2 \pm 0.3
$\lambda = 64.0\%$	91.3 \pm 0.2	91.5 \pm 0.3	91.9\pm0.3
$\lambda = 40.9\%$	90.6 \pm 0.4	90.8 \pm 0.5	91.1\pm0.7
$\lambda = 32.8\%$	90.2 \pm 0.5	90.5 \pm 0.8	90.8\pm0.6
$\lambda = 26.2\%$	89.8 \pm 0.8	90.3 \pm 0.7	90.7\pm0.9
$\lambda = 13.4\%$	89.2 \pm 0.8	89.7 \pm 0.9	90.4\pm0.8
$\lambda = 8.59\%$	84.5 \pm 0.9	86.1 \pm 1.0	87.0\pm0.7
$\lambda = 5.72\%$	76.9 \pm 1.1	78.4 \pm 1.4	79.2\pm1.3

Table 9: Performance (top-1 test accuracy \pm standard deviation) of pruning VGG-19 on CIFAR-10 using Global Gradient with and without AP. The hyper-parameters and the LR schedule are from (Frankle and Carbin 2019).

(i) Params: 1.1M; (ii) Train Steps: 300 epochs; (iii) Batch size: 256; (iv) LR Schedule: warmup to 0.1 at 150 epochs, 10X drop at 150, 240 epochs.			
Percent of Weights Remaining	LAMP	AP-Lite	AP-Pro
$\lambda = 100.0\%$	74.6 \pm 0.5	74.6 \pm 0.5	74.6 \pm 0.5
$\lambda = 64.0\%$	73.4 \pm 0.6	73.7 \pm 0.5	74.2\pm0.6
$\lambda = 32.8\%$	71.5 \pm 0.7	71.9 \pm 0.8	72.2\pm0.7
$\lambda = 26.2\%$	69.6 \pm 0.8	70.3 \pm 0.7	71.1\pm0.7
$\lambda = 13.4\%$	65.8 \pm 0.9	66.6 \pm 0.7	68.8\pm0.9
$\lambda = 5.72\%$	61.2 \pm 1.4	62.2 \pm 1.2	63.5\pm1.5

Table 10: Performance (top-1 test accuracy \pm standard deviation) of pruning DenseNet-40 on CIFAR-100 using Layer-Adaptive Magnitude Pruning (LAMP) (Lee et al. 2020) with/without AP. The hyper-parameters and the LR schedule are from (Zhao et al. 2019).

(i) Params: 2.36M; (ii) Train Steps: 200 epochs; (iii) Batch size: 128; (iv) LR Schedule: warmup to 0.1 at 60 epochs, 10X drop at 60, 120, 160 epochs.			
Percent of Weights Remaining	LAP	AP-Lite	AP-Pro
$\lambda = 100.0\%$	73.7 \pm 0.4	73.7 \pm 0.4	73.7 \pm 0.4
$\lambda = 64.0\%$	72.5 \pm 0.4	72.7 \pm 0.3	72.9\pm0.5
$\lambda = 32.8\%$	72.1 \pm 0.8	72.5 \pm 0.9	72.8\pm0.7
$\lambda = 26.2\%$	70.5 \pm 0.9	70.9 \pm 0.8	71.4\pm0.8
$\lambda = 13.4\%$	67.3 \pm 0.8	68.2 \pm 1.2	69.1\pm0.8
$\lambda = 5.72\%$	64.8 \pm 1.5	66.2 \pm 1.5	67.4\pm1.1

Table 11: Performance (top-1 test accuracy \pm standard deviation) of pruning MobileNetV2 on CIFAR-100 using Lookahead Pruning (LAP) (Park et al. 2020) with/without AP. The hyper-parameters and the LR schedule are from (Chin et al. 2020).

(i) Params: 25.5M; (ii) Train Steps: 90 epochs; (iii) Batch size: 1024; (iv) LR Schedule: warmup to 0.4 at 5 epochs, 10X drop at 30, 60, 80 epochs.			
Percent of Weights Remaining	IMP	AP-Lite	AP-Pro
$\lambda = 100.0\%$	77.0 \pm 0.1	77.0 \pm 0.1	77.0 \pm 0.1
$\lambda = 64.0\%$	77.2 \pm 0.2	77.5 \pm 0.1	77.7\pm0.1
$\lambda = 32.8\%$	76.8 \pm 0.2	77.2 \pm 0.3	77.5\pm0.4
$\lambda = 26.2\%$	76.4 \pm 0.3	76.9 \pm 0.4	77.2\pm0.3
$\lambda = 13.4\%$	75.2 \pm 0.4	76.1 \pm 0.3	76.8\pm0.6
$\lambda = 8.59\%$	73.8 \pm 0.5	75.2 \pm 0.7	75.9\pm0.5
$\lambda = 5.72\%$	71.5 \pm 0.4	72.6 \pm 0.5	73.5\pm0.4

Table 12: Performance (top-1 test accuracy \pm standard deviation) of pruning ResNet-50 on ImageNet using Iterative Magnitude Pruning (IMP) with and without AP (Frankle and Carbin 2019). The hyper-parameters and the LR schedule are from (Renda, Frankle, and Carbin 2019).

(i) Params: 86M; (ii) Train Steps: 50 epochs; (iii) Batch size: 1024; (iv) Optimizer: Adam; (v) LR Schedule: cosine decay from 1e-4.			
Percent of Weights Remaining	IMP	AP-Lite	AP-Pro
$\lambda = 100.0\%$	98.0 \pm 0.3	98.0 \pm 0.3	98.0 \pm 0.3
$\lambda = 64.0\%$	98.4 \pm 0.3	98.5 \pm 0.2	98.7\pm0.3
$\lambda = 32.8\%$	97.3 \pm 0.6	98.0 \pm 0.4	98.2\pm0.6
$\lambda = 26.2\%$	96.8 \pm 0.7	97.3 \pm 0.7	97.6\pm0.5
$\lambda = 13.4\%$	88.1 \pm 0.9	89.9 \pm 0.6	91.1\pm0.8
$\lambda = 8.59\%$	84.4 \pm 0.8	85.5 \pm 0.8	87.4\pm0.7
$\lambda = 5.72\%$	82.1 \pm 0.9	83.6 \pm 0.8	84.8\pm1.0

Table 13: Performance (top-1 test accuracy \pm standard deviation) of pruning Vision Transformer (Dosovitskiy et al. 2020) (ViT-B-16) on CIFAR-10 using IMP with and without AP (Frankle and Carbin 2019). The hyper-parameters and the LR schedule are from (Dosovitskiy et al. 2020).

B.3 Ablation Study Results using VGG-19

In this section, we repeat the ablation study experiment in the Section of Ablation Study (i.e., Section 4.3) using VGG-19 on CIFAR-10 with the Global Gradient method. We note that the hyper-parameters and the LR schedule used are from (Frankle and Carbin 2019).

As show in Table 14, we observe similar performance trends as Table 7. Specifically, the performance of AP-Lite-NO-WR is much lower as compared to AP-Lite, suggesting the effectiveness of weight rewinding (WR). Furthermore, when AP works solely, the performance (i.e., AP-Lite-SOLO) tends to become much worse than AP-Lite. This agrees with our argument that AP does not work solely as it does not evaluate the importance of weights. Instead, the goal of AP is to work in tandem with existing pruning methods and aims to improve their performance by reducing the dynamic DNR.

λ	64%	51.2%	40.9%	32.8%
AP-Lite	91.7 ± 0.3	90.6 ± 0.5	89.8 ± 0.9	89.5 ± 0.8
AP-Lite-SOLO	90.5 ± 0.7	89.8 ± 0.6	88.3 ± 1.1	87.2 ± 1.3
AP-Lite-NO-WR	90.8 ± 0.4	90.1 ± 0.3	88.5 ± 0.9	87.7 ± 1.0

Table 14: Ablation Study: Performance Comparison (top-1 test accuracy ± standard deviation) between AP-Lite and AP-SOLO, AP-Lite-NO-WR on pruning VGG-19 using the CIFAR-10 dataset via Global Gradient. The hyper-parameters and the LR schedule are from (Frankle and Carbin 2019).

B.4 Pruning Rate of AP, q

In this subsection, we repeat the experiments of pruning ResNet-20 on CIFAR-10 using Global Magnitude and AP-Lite. We note that the overall pruning rate is fixed as 20% and the pruning rate of AP increases from 1% to 5%. Correspondingly, the pruning rate of Global Magnitude decreases from 19% to 15%. The experimental results are summarized in Table 15. We observe that as we increase the pruning rate of AP from 2%, the performance tends to decrease. Similar performance trends can be observed using VGG-19 on CIFAR-10 as well (see Table 16). As an example, in Table 16, the top-1 test accuracy is reduced from 88.5 to 87.1 for $\lambda = 26.2\%$ when the value of q increases from 2% to 5%. It suggests that the primary goal of pruning still should be pruning less important weights.

The theoretical determination of the optimal value of q is clearly worth deeper thought. Alternatively, q can be thought of as a hyper-parameter and tuned via the validation dataset and let $q = 2$ could be a good choice as it provides promising results in various experiments.

AP Pruning Rate, q	1%	2%	3%	5%
AP-Lite ($\lambda = 64.0\%$)	89.8 ± 0.1	90.0 ± 0.2	89.5 ± 0.4	89.2 ± 0.6
AP-Lite ($\lambda = 40.9\%$)	88.2 ± 0.4	88.9 ± 0.6	88.5 ± 0.7	87.3 ± 0.5
AP-Lite ($\lambda = 26.2\%$)	87.1 ± 0.5	87.9 ± 0.8	86.7 ± 0.8	86.3 ± 0.9

Table 15: Performance (top-1 test accuracy ± standard deviation) of AP-Lite when iterative pruning ResNet-20 on CIFAR-10 with different pruning rate.

AP Pruning Rate, q	1%	2%	3%	5%
AP-Lite ($\lambda = 64.0\%$)	91.1 ± 0.2	91.7 ± 0.3	90.2 ± 0.5	89.8 ± 0.6
AP-Lite ($\lambda = 40.9\%$)	88.7 ± 0.5	89.8 ± 0.9	89.3 ± 1.1	88.0 ± 0.9
AP-Lite ($\lambda = 26.2\%$)	87.9 ± 0.8	88.5 ± 0.7	88.1 ± 1.3	87.1 ± 1.3

Table 16: Performance (top-1 test accuracy ± standard deviation) of AP-Lite when iterative pruning VGG-19 on CIFAR-10 with different pruning rate.

B.5 Effect of AP on Dynamic DNR

In this section, we repeat the same experiments in the Section of Performance Evaluation (i.e., Section 4) and compare the dynamic DNR with and without using AP-Lite in Tables 18 & 17.

In Table 18, we observe that dynamic DNR is reduced from 9.8% to 9.1% at $\lambda = 80\%$ after applying AP-Lite with a pruning rate of 2%. As λ decreases, AP-Lite also works well and reduces dynamic DNR from 5.1% to 4.4% at $\lambda = 20.9\%$. Similar performance trends can also be observed in Table 17. This suggests that AP works as expected and explains why AP is able to improve the pruning performance of existing pruning methods.

λ	80%	51.2%	40.9%	32.8%	26.2%	20.9%
Global Magnitude	7.7%	7.4%	7.0%	6.7%	6.3%	6.1%
AP-Lite (2%)	7.3%	7.1%	6.8%	6.3%	5.9%	5.5%

Table 17: The dynamic DNR when iteratively pruning ResNet-20 on CIFAR-10 using Global Magnitude and AP-Lite (with a pruning rate of 2%).

λ	80%	51.2%	40.9%	32.8%	26.2%	20.9%
Global Gradient	9.8%	9.2%	7.6%	7.0%	5.8%	5.1%
AP-Lite (2%)	9.1%	8.6%	7.0%	6.1%	4.9%	4.4%

Table 18: The dynamic DNR when iteratively pruning VGG-19 on CIFAR-10 using Global Gradient and AP-Lite (with a pruning rate of 2%).